Research Square

Preprints are preliminary reports that have not undergone peer review.
They should not be considered conclusive, used to inform clinical practice,
or referenced by the media as validated information.

Urban Meander Loop Dynamics and Future Projections – Insights from the Barak River, India

Wajahat Annayat

Wajahatannayat123@gmail.com

National Institute of Technology Srinagar https://orcid.org/0000-0001-6551-2814

Research Article

Keywords: Arima Model, Barak River, Geomorphological Change, Land use and land cover (LULC), Meander Loop

Posted Date: September 2nd, 2025

DOI: https://doi.org/10.21203/rs.3.rs-7386690/v1

License: This work is licensed under a Creative Commons Attribution 4.0 International License. Read Full License

Version of Record: A version of this preprint was published at Acta Geophysica on April 6th, 2026. See the published version at https://doi.org/10.1007/s11600-026-01864-x.

Abstract

The Barak River is recognised as one of the most highly meandering rivers in Northeast India, which presents considerable challenges for local communities, particularly during flood events. This study conducts a thorough investigation into the geomorphological transformations occurring within an urban meander loop situated in the centre of Silchar city, Assam, India. The analysis demonstrates that the length, width, ratio, and wavelength of the meander have exhibited an overall increase, while the sinuosity and radius of curvature have shown a declining trend. A comprehensive land use and land cover analysis of the urban meander loop reveals a significant increase in settlements by 16.18%, accompanied by reductions in water bodies (0.57%), dense vegetation (2.58%), and agricultural land (13.16%). The Auto Regressive Integrated Moving Average (ARIMA) model was employed to facilitate predictive analysis to forecast channel shifting trends up to the year 2030. The results indicate that the channel in the urban meander loop is undergoing erratic changes, shifting either to the right or left. There is a high correlation between the observed and the predicted values, with an R^2 value of 0.8. The persistent uncertainty in channel movements is anticipated to pose ongoing threats to nearby settlements and significantly alter existing land use in the foreseeable future.

1. Introduction

The term "meander" itself has historical origins. It derives from the ancient name "Maiandros," referencing a deity in Greek mythology believed to alter territorial boundaries along riverbanks, often resulting in legal disputes (da Silva et al. 2017). Due to their dynamic nature, meandering rivers have long posed challenges and have thus drawn the attention of scientists since the late 19th century. Foundational contributions were made by researchers Friedkin (1945), but a significant shift occurred in the latter half of the 20th century, following the work of Rozovskii (1957). Early research often relied on physical models and flume experiments to understand river channel behaviour. Although preliminary attempts at quantifying meander parameters date back to the 1930s, it wasn't until the 1960s that researchers began developing empirical formulas and exploring interrelationships among meandering variables (Leopold & Wolman, 1957; Leopold & Langbein, 1966). The 1970s saw a shift towards analysing meandering behaviour over short time scales, opening new research avenues (Daniel, 1971; Lewin & Brindle et al., 1977; Hooke et al., 1983; Ferguson, 1984). Howard et al. (1994) later advanced the field by developing computational models for simulating river dynamics. Lewin and Brindle et al. (1977) employed a straightforward method of overlaying temporal photographs to visually assess channel changes. Hooke et al. (1983) classified five different methodologies for analysing meanders, three of which involve comparing river reaches across different periods. Experimental and field studies consistently show that alluvial river meanders gradually migrate downstream (Tiffany et al., 1939; Friedkin, 1945; Ackers & Charlton, 1970). Hickin (1977) observed that meanders in freely migrating, unconfined systems tend to exhibit more significant movement compared to those in more stable, resistant terrains. Despite diverse distortions in meander patterns, consistent trends often emerge within a given channel. Klaassen and Masselink (1993) analysed meandering progression by superimposing sine curves onto river paths and identified five development modes, like expansion, rotation, translation, and their combinations.

Meandering rivers have played a crucial role in supporting human civilisation by providing essential resources such as water for domestic use, agriculture, and transport, while simultaneously sustaining diverse riparian and aquatic ecosystems. However, due to their highly dynamic and unpredictable nature, meandering channels present numerous practical challenges in management and planning (Inglis and Lacey, 1947; Jansen et al., 1979; Martín-Vide, 2006). There have been various explanations put forward regarding why rivers meander. They include the Excess Energy theory (Inglis and Lacey, 1947; Leopold & Wolman, 1960), Earth Rotation theory (Gilbert, 1884), Disturbance theory (Friedkin, 1945), and Helicoidal Flow theory (Onishi et al., 1976). Yet, even with a vast amount of research, the causes of meandering are still very complicated, and no one theory provides a comprehensive explanation for all the observed behaviours. Understanding river behaviour requires detailed knowledge of streamflow characteristics and their interaction with channel geometry and planform, which are pivotal in river engineering and fluvial geomorphology (Thorne et al., 1997). Water in the meandering channels flows in a spiralling manner and, as a result, is not only accelerated in the outer concave side but is also guided through centrifugal forces, which is an important factor in erosion of such points. This has been expounded by Knighton (1998) and also observed by Chang (1988), who covered such phenomena as the super-elevation of the water surface at the outer bank, flow circulation between the inner and outer bend and also the interaction of linear and rotational forces leading to spiral movement along the bends.

The process of river meandering is fundamentally driven by bank erosion, which leads to lateral migration and eventual channel shift. As the banks erode and migrate sufficiently, the river may eventually loop back on itself, forming a cut-off. Two primary types of cut-offs are identified in fluvial literature: chute and neck cut-offs Thorne et al., 2020). Chute cut-offs generally occur across stretches longer than the width of the river channel and are more frequently observed, whereas neck cut-offs form across narrower segments of the floodplain and are relatively uncommon Ondruch et al., 2002). A notable long-term study by Hooke (2007), based on two decades of observations of a naturally active meandering river, shed light on the geomorphological instability and evolution of such systems. Findings indicated that as sinuosity increases, so does the lateral migration rate of the channel. However, when the meander becomes excessively sinuous, with large bend amplitudes, the river’s transport efficiency, slope, and velocity tend to decline. Once a certain threshold of sinuosity is reached, the river may no longer sustain its form, leading to the formation of a cut-off. Such events reduce sinuosity but result in increased slope and flow velocity. Therefore, in alluvial plains, the process of meandering is ongoing and seldom reaches a point of complete stability. In one prominent study, Takagi et al. (2007) investigated both the spatial and temporal changes in the conveyance of the large, sandy, braided environment of the Brahmaputra River with the help of satellite images as well as geographic information systems (GIS). In studying the characteristics of meandering regarding any notable avulsion activities on the Ganga River, Roy and Sinha (2018) examined the morphodynamics of meandering. In their study, the parameters related to the channel sinuosity were pointed out to be strongly

correlated with the sediment dynamics. In the same light, Methun Deb and Dabojani Das (2012) evaluated the meandering properties of the Manu River in Bangladesh through remote sensing and the utilisation of GIS. These shark researchers compared contemporary satellite images with past data to identify how meander parameters have changed with time. Interestingly, they found that their results are non-linear, where initially there was an increase in channel sinuosity after which it decreased in later years. During recent years, an increasing amount of attention has focused on the study of the human impact on the morphology of rivers, especially in view of the meander development and channel dynamics (Sil et al., 2022; Annayat et al., 2022; Debnath et al., 2023; Khan et al., 2025)

This paper discusses geomorphological changes in one of the most dynamic urban meander loops of the Barak River in Silchar, Assam, in India. The variation over time in channel behaviour was analysed by quantifying such important meander parameters as length, width, ratio, wavelength, sinuosity and radius of curvature using historical satellite imagery. Analysis of land use and land cover (LULC) demonstrated significant growth in land cover of settlements and a reduction in the area covered by agricultural land, dense vegetation and waterbodies. Data were observed over time to determine the Auto-Regressive Integrated Moving Average (ARIMA) model to forecast channel migration. The model is used to forecast the most likely future channel locations up until the year 2030, which would act as imperative information during urban planning and the areas of flood risk management. The following points are the central objectives of this study.

I. To identify the geomorphological changes of the urban-meander loop of River Barak at Silchar, Assam, through the evaluation of dominant parameters of meandering (meander length, width, ratio, wavelength, sinuosity and radius of curvature).

II. To understand the transformation of land use and land cover (LULC) of the urban meander loop area longitudinally with the ultimate goal of measuring the sprawling of urban growth area and reduction of natural land types, i.e., waterbodies, vegetation, and agricultural land.

III. To predict the possibilities of channel changes until the year 2030, through ARIMA model outputs to aid flood risk reduction and urban design within the city of Silchar.

2. Regional Setting

The Barak River stands as the second-largest river system in Northeast India, flowing almost parallel to the Brahmaputra River in the southeastern segment of the Himalayan foothills. It spans approximately 1.38% of India's total geographical area (Jain et al., 2007). Originating from the Japvo mountain in the Manipur hills at an altitude of 3,015 meters, the Barak River initially flows southward through rugged hilly terrain until it reaches Tipaimukh, a location near the tri-junction of Assam, Manipur, and Mizoram. At this juncture, the river takes a sharp bend and transitions into the plains of Assam's Cachar district, briefly forming the boundary between Assam and Manipur near Jirimat, just upstream of Lakhimpur. The river then continues its westward journey through the Barak Valley before crossing into Bangladesh, where it bifurcates into the Surma and Kushiyara rivers, eventually merging into the Meghna River. The area selected for this study lies in the main Silchar city Ghat in Assam (Fig. 1). Geographically, the basin is situated between latitudes 22°44'N and 25°58'N and longitudes 89°50'E and 94°00'E. The river features a gentle bed slope, which decreases downstream from approximately 1:10,000 in its upper reaches to about 1:20,000 in the lower sections (Jain et al., 2007). Along the alluvial floodplains, riparian vegetation is relatively sparse. Dominant plant communities include bamboo thickets (Bambusoideae), both wet and dry grasslands (Phragmites karka), and savanna grasslands (Apluda mutica) (Annayat et al, 2020a, b). Climatically, the basin experiences a warm and humid subtropical environment, receiving annual rainfall between 2,500 mm and 4,000 mm, with over 80% occurring during the monsoon months from April to October (Annayat 2025).

3. Data Used

Based on the scope of this study, multiple datasets (1984, 1992, 2002, 2012, and 2017) were utilised to examine the geomorphological transformation of the Barak River's urban meander loop within Silchar city. High-resolution satellite imagery was utilised to extract meander parameters, including length, width, wavelength, meander ratio, sinuosity, and radius of curvature, over various periods. These spatial datasets enabled the detection of morphological changes in the river channel. Also, remote sensing methods analysed land use and land cover (LULC) information (2000, 2010, 2020) to determine the changes in the settlement, agricultural lands and vegetation, and waterbodies within the region. The ARIMA model had time series data input based on the above analyses, and it was used to conclude on the future trend of channel migration until the year 2030. A combination of spatial, temporal and statistical data sets gave a broad foundation upon which to assess the historical trends and future projection of changes in the behaviour of the river. Table 1 displays all the information regarding the information that was utilised in the current study.

Table 1
Summary of datasets, sources, and parameters used for assessing geomorphological changes and predicting future channel migration of the Barak River's urban meander loop within Silchar city

Satellite	Sensor	Path/ Row	Scale	Year	Source
Geomorphological Data (Landsat Images 1,2, 5, 7, 8)	MSS, TM, ETM^{+}, ETM, OLI	136/43	60m and 30 m	1984, 1992, 2002, 2012, 2017	http://earthexplorer.usgs.gov
LULC Data	ETM^{+}, ETM, OLI	136/43	30 m	2000, 2010, 2020	http://earthexplorer.usgs.gov

3. Methodology

The methodology adopted in this study is structured into two primary components: (i) morphometric parameters of individual meander loops were assessed across five timeframes (1984, 1992, 2002, 2012, and 2017), and LULC analysis was carried out for the years 2000, 2010 and 2020; (ii) prediction using the ARIMA time-series model. Each of these components contributes uniquely to understanding the geomorphological transformation and future trajectory of the urban meander loop in Silchar.

3.1. Morphometric Analysis

In this study, the initial data processing, Landsat 1 (MSS) imagery exhibited line striping, a scanning-related error. This issue was rectified through appropriate filtering techniques as suggested by Pan and Chang (1992). The original 60-meter resolution MSS data was georeferenced using multiple ground control points to enhance spatial accuracy, and subsequently resampled to a finer 30-meter resolution. Additionally, radiometric and haze corrections were performed using ERDAS IMAGINE 14, following the procedures outlined by Hazarika et al. (2015). The river channel has also been divided into two reaches to study the pattern of migration, where these two reaches are around the Silchar town. These reaches were not perfectly regularly spaced, as there were specific visual readings that informed their location using several images of multi-temporal satellite images. The denser segmentation has been used in regions with strong morphometric change, which makes it more realistic in depicting dynamic river behaviour.

3.2 ARIMA Model

The Autoregressive Integrated Moving Average (ARIMA) model was used in attempting to predict the future trend of migration in the looped urban meander of the Barak River at the Silchar site. ARIMA is one of the common models of time-series forecasting and incorporates three elements, are: an Autoregression (AR), differencing (I), and moving average (MA). Autoregressive (AR) component linearises the current value of a series in terms of the past values of the series. That of an AR model of order p is written generally as:

$y_t = C + \phi_1 y_{t-1} + \phi_2 y_{t-2} + \cdots + \phi_p y_{t-p} + \epsilon_t$ (1)

Where:

y_t is the value at time *t*, C is a constant,

ϕ_1, $\phi_2 \ldots \phi_p$ are the AR coefficients, and

ϵ_t is the error term at time *t*.

The Moving Average (MA) component captures the dependency between an observation and a residual error from a moving average model applied to lagged observations. The MA model of order *q* is given by:

$y_t = C + \epsilon_t - \theta_1 \epsilon_{t-1} - \theta_2 \epsilon_{t-2} - \cdots - \theta q \epsilon_{t-q}$ (2)

Where:

θ_1, $\theta_2 \ldots$, θq are the MA coefficients,

ϵ_t and its lags are white noise error terms.

Combining both AR and MA components results in the ARMA (p, q) model, represented as

$y_t = C + \phi_1 y_{t-1} + \phi_2 y_{t-2} + \cdots + \phi_p y_{t-p} + \epsilon_t - \theta_1 \epsilon_{t-1} - \theta_2 \epsilon_{t-2} - \cdots - \theta_q \epsilon_{t-q}$ (3)

In this study, the ARIMA model was applied after differencing the data to ensure stationarity, making it suitable for time-series forecasting. The predicted values of channel migration trends up to the year 2030 were obtained using this model.

4. Results and Discussion

4.1 Morphometric Parameters and LULC analysis

Based on morphometric analysis, several parameters, such as meander length, width, ratio, sinuosity, wavelength, and radius of curvature, were examined across different periods. As shown in Fig. 2, the longest meander was recorded in 2002 at reach-1 (Neairgram Part-II), measuring 5,496 meters, while the shortest was observed at reach-2 (Gangapur) in 2012, with a length of 2,369 meters. The average meander length between 1984 and 2017 shows a rising trend. Comparable findings have been reported for the Manu River in Bangladesh (Mithun et al., 2012) and the Bhagirathi River in West Bengal (Islam and Guchhait, 2017). Figure 3 illustrates that the widest meander, 3,054 meters, occurred in 2002 at reach-1 (Neairgram Part-II), whereas the narrowest, at 2,657 meters, was found in 2012 at reach-2 (Gangapur). The average width of the meanders during the study period also demonstrates an upward trend. As indicated in Fig. 4, the highest meander ratio (1.12) was noted in 2012 at reach-2 (Gangapur), and the

lowest (0.55) in 2002 at reach-1 (Neairgram Part-II), again reflecting an overall increasing pattern. Figure 5 highlights that the maximum sinuosity value of 2.15 was observed in 2017 at reach-1 (Neairgram Part-II), while the minimum, 1.56, occurred in 2002 at reach-2 (Gangapur). Notably, both the reaches (reach-1, reach 2) displayed sinuosity values greater than 1.5, suggesting the presence of highly sinuous channel segments. Leopold and Wolman (1957) noted that channels with sinuosity greater than 1.5 are classified as meandering. The values obtained in this study fall within the range reported by earlier works, such as Debnath et al. (2017), Bag et al. (2019), and Mithun et al. (2012). Figure 6 illustrates the variation in wavelength values for Neairgram Part-II and Gangapur over the years 1984, 1992, 2002, 2012, and 2017. Gangapur consistently recorded higher wavelength values across all five years, maintaining a relatively stable level slightly above 4500 meters. Contrastingly, Neairgram Part-II has a significant decrease observed between 1984 and 2012, peaking in 2012, and rising further in 2017. This implies that Neairgram Part-II might show deviation on the negative scale in terms of its wavelength over the years, but latterly improving at the end, whereas Gangapur wavelength was consistent throughout the observation period. In Fig. 7, the radius of curvature of Neairgram Part-II and Gangapur has been illustrated regarding 1984, 1992, 2002, 2012 and 2017. In the whole interval, there was a continued greater radius of curvature in Neairgram Part II than in Gangapur. The Neairgram Part-II values were highest in 2002, and there was a minimal variation of values in the remaining years, with a regressive value in 2012 and a stagnated value in 2017. Gangapur, on the other hand, had relatively small and constant reimbursement rates every year except for slight fluctuations. This trend indicates that Neairgram part-II showed bigger changes of curvature over the years than Gangapur, which has revealed a slight variation.

Figure 8 (a, b) shows a map that tracks the positional changes of a river channel over time from 1984 to 2017. For reach-1, each year is represented by a different colour—magenta for 1984, yellow for 1992, black for 2002, cyan for 2012, and red for 2017. From the pattern, it's evident that the river has undergone noticeable lateral shifting, especially towards the eastern side over time. The red line, representing 2017, shows a clear outward movement compared to earlier years, indicating erosion on one bank and deposition on the other. For reach – 2, each year's river path is marked with a different colour: light pink for 1984, red for 1992, black for 2002, green for 2012, and dark pink for 2017. The river shows significant lateral movement and channel migration across the years, especially noticeable in the bends and curves of the channel. The most recent channel path (2017) lies further outward in some segments compared to earlier years, indicating gradual erosion and deposition processes.

The land use and land cover (LULC) dynamics between 2000 and 2020 reveal significant transformations within the study area (Table 2 and Fig. 9). Agricultural land has experienced the most substantial decline, decreasing from 34.60 km² in 2000 to 21.44 km² in 2020, reflecting a net reduction of approximately 13.16%. Dense vegetation also declined steadily, with its area shrinking from 13.61 km² to 11.03 km² over the same period, marking a 2.58% decrease. Water bodies showed fluctuations, increasing slightly in 2010 before reducing to 7.61 km² in 2020, resulting in an overall net loss of 0.57%. Conversely, the settlement category has expanded significantly, growing from 18.34 km² in 1999 to 34.52 km² in 2020, indicating rapid urbanisation with a net increase of 16.18%. The "Others" category remained relatively stable, with a marginal rise of 0.13%. These changes highlight a clear trend of urban expansion occurring at the expense of agricultural and vegetated areas.

The accuracy assessment of the classified LULC maps for the years 2000, 2010, and 2020 reflects high classification reliability across all categories (Table 3). In 2000, the user’s accuracy exceeded 94% for all land cover types, with water bodies and dense vegetation achieving particularly high accuracies of 98.5% and 98.9%, respectively. The producer’s accuracy for the same year was also impressive, with agricultural land reaching 100% and an overall accuracy of 95.14%. In 2010, although there was a slight drop in some categories, the results remained strong, with settlement and agricultural land showing consistent accuracy values. The overall accuracy for 2010 stood at 96.32%, indicating dependable classification. In 2020, the classification quality improved again, with users’ accuracy for water bodies and dense vegetation at 98.3% and 95.86%, respectively, while settlements reached 95.68%. The producer’s accuracy was similarly high, notably 100% for the “Others” class and over 93% for most other categories. The overall accuracy for 2020 was 98.51%, confirming the robustness and reliability of the LULC classification across all three time periods.

Table 2
Area statistics of LULC

LULC Class	Area in Km^2			Net Change in %
	2000	2010	2020	
Waterbodies	8.181	9.4176	7.6078	-0.5732
Dense Vegetation	13.6109	12.9789	11.0277	-2.5832
Agricultural Land	34.5994	25.209	21.4436	-13.1558
Settlement	18.3375	27.5157	34.5173	16.1798
Others	1.7991	1.4067	1.9315	0.1324

Table 3: Accuracy Assessment

User's Accuracy						Producer's Accuracy					Overall Accuracy
Year	Water Bodies	Dense Vegetation	Agricultural Land	Settlement	Others	Water Bodies	Dense Vegetation	Agricultural Land	Settlement	Others	
2000	98.5	98.9	98.3	94.9	96.1	99.7	99	100	96.11	99.3	95.14
2010	96.8	94	96.3	94.95	99	97.5	98.5	96.5	98.2	93.83	96.32
2020	98.3	95.86	93.2	95.68	100	96.2	96.9	93.21	95.8	91.74	98.51

4.2 Migration Rates and Processes

An analysis of the morphometric characteristics at Neairgram Part-II and Gangapur for the years 1984 to 2017 reveals gradual yet noticeable changes in channel width and curvature. At Neairgram Part-II, the channel width increased from 340 meters in 1984 to a peak of 439 meters in 2012, before slightly narrowing to 400 meters in 2017 (Table 4). Meanwhile, the radius of curvature remained relatively consistent, fluctuating modestly between 1064 and 1238 meters. The ratio of radius of curvature to channel width (r_c/b) shows a gradual decline from 3 in 1984 to 2.4 in 2012, comparable with the results reported by Nanson and Hickin (1986) ($r_c/b \sim 2–3$), suggesting a subtle straightening of the channel over time. A similar trend is observed in Gangapur, where the channel width initially increased significantly from 360 meters in 1984 to 508 meters in 1992, followed by a gradual reduction to 450 meters by 2017 (Table 4). The radius of curvature remained fairly stable, resulting in rc/b ratios ranging from 1.3 to 1.1. These trends indicate a shift toward more uniform and potentially more stabilised meander bends, influenced by both natural fluvial processes and possibly anthropogenic factors, within relatively stable catchment areas of 19274 km² and 18677 km², respectively.

Table 4
Temporal variation in channel width, radius of curvature, and their ratio for two meander reaches (Neairgram Part II and Gangapur) of the Barak River across different years.

Location	Year	Channel Width b (m)	Radius of curvature r_c (m)	Ratio r_c / b
Neairgram Part II	1984	340	1050	3.0
	1992	361	1013	2.8
	2002	405	1238	3.0
	2012	439	1055	2.4
	2017	400	1064	2.6
Gangapur	1984	360	492	1.3
	1992	508	524	1.0
	2002	490	498	1.0
	2012	458	474	1.0
	2017	450	498	1.1

4.3 Centerline channel shifting using ARIMA Model

The cross-sectional analysis of the riverbank migration across various sections from 1984 to projected values for 2030 demonstrates dynamic lateral shifts on both left and right banks (Table 5 and Fig. 10). CS-1 experienced a gradual increase in right bank migration from 24 meters (1984–1992) to 52.03 meters by 2030, with moderate accuracy as shown by an RMSE of 2.57 and R^2 of 0.83. CS-2 displayed significant early right bank migration, peaking at over 318 meters by 2002, followed by a transition toward left bank activity post-2017, indicating a notable shift in fluvial behaviour. CS-3 also recorded consistent right bank erosion, increasing to nearly 80 meters by 2030, while CS-2 presented a less consistent pattern, with predominantly left bank migration showing a dip in 2017 before rising again. CS-5 revealed a sharp and steady right bank migration, intensifying to over 140 meters in the projected period, reflecting one of the most active zones. Lastly, CS-6 exhibited significant right bank migration until 2017, followed by a reversal toward the left bank in later years. Overall, CS-2 and CS-6 showed the highest migration magnitudes and model uncertainty, as evident from their higher RMSE and BIC values. The data suggest that river dynamics in these reaches are influenced by localised factors such as bank composition, flow variability, and anthropogenic pressure.

Table 5
Bankline migration distances (in meters) for selected cross-sections in Reach 1 and Reach 2 of the study area during different time intervals, indicating the migrating bank side (R.B = Right Bank, L.B = Left Bank), along with model performance statistics (RMSE, R^2, and BIC)

Cross-Section	1984–1992	1984–2002	1984–2012	1984–2017	2017–2023	2023–2030	RMSE	R^2	BIC
CS-1(Reach 1)	24(R.B)	11.27(R. B)	34.90(L. B)	43.43(R. B)	48.31(R. B)	52.03(R. B)	2.57	0.83	2.82
CS-2(Reach 1)	263(R. B)	207(R. B)	318.01(R. B)	273.69(R. B)	243.08(L. B)	230.07(L. B)	12.62	0.84	4.44
CS-3(Reach 1)	33(R.B)	18.36(L. B)	58.33(R. B)	60.73(L. B)	68.90(R. B)	79.96(R. B)	3.14	0.82	2.16
CS-4(Reach 2)	20(L.B)	16.6(R. B)	21(L.B)	7.87(L. B)	5.3(L. B)	21.5(L. B)	2.73	0.67	4.10
CS-5 (Reach 2)	23(L.B)	14.76(R. B)	35.6(R. B)	61.79(R. B)	94.93(R. B)	140.01(R. B)	3.42	0.89	2.31
CS-6(Reach 2)	154.3(R. B)	127.34(R. B)	184.96(R. B)	190.23(R. B)	184.36(L. B)	175.94(L. B)	10.07	0.73	4.42

5. Discussion

The Barak River, flowing through the urban stretch of Silchar, exhibits noticeable geomorphological alterations over the past few decades. The analysis of channel metrics, such as meander length, width, ratio, wavelength, and sinuosity, indicates a significant shift in river dynamics. An increasing trend in meander length and width, along with decreasing sinuosity and radius of curvature, suggests the river is undergoing lateral expansion with a tendency toward straightening. This transformation could be attributed to hydrological fluctuations, anthropogenic encroachments, and sediment dynamics in the urban environment. Hooke and Harvey (1983) reported meander lengths of 500–3500 m in the River Dane, while Lauer and Parker (2008) observed lengths of 800–4500 m and widths of 600–3200 m in the Mississippi River. The present study shows comparable results, with meander lengths ranging from 2369 to 5496 m, reflecting the influence of both natural and human factors. The influence of urbanisation on the morphology of rivers is also supported by the Land Use and Land Cover (LULC) analysis taking place between 2000 and 2020. There is considerable settlement expansion of 16.18% as a serious sign of urban sprawl in the floodplain, especially at the cost of agricultural land, that reduced by more than 13%. The dense vegetation and water bodies also experienced marginal losses, which implied that there was stress on the ecosystem because of human interference. The reliability of the analysis was confirmed in the accuracy analysis of the years-LULC, with overall accuracies being recorded at all instances as greater than 95% (Congalton & Green, 2009). It is only in the measurement of channel width and radius of curvature at two very prominent sites, Neairgram Part II and Gangapur, that constant changes can be identified. Although the channel width has slowly got wider over the years, the ratio of the radius of curvature to channel width has gradually deteriorated, pointing to tight turning angles and bank stability (Leopold & Wolman, 1960; Hooke, 2007). Although there is a constant catchment area, geomorphological adaptation is indicated by local channel alterations due to the natural and anthropogenic processes. Moreover, the analysis of morphological parameters consisting of sinuosity (C), meander ratio (MR), wavelength, and radius of curvature (RC) between 1984 and 2017 observes variations occurring in various reaches. Simple rotation without extreme modifications on the planform geometry is observed in some reaches, whereas there are slight changes in width and curvature, and this means gradual but subtle morphodynamic development. These shifts are also in line with the localised effects, including floodplain confinement, developments in infrastructure and flood fluctuations. The cross-sectional analysis from 1984 to projected values for 2030 demonstrates spatially uneven lateral migration. Sections such as CS-1, CS-3, and CS-5 recorded progressive right bank migration, while CS-2 and CS-6 showed complex behaviour with migration initially concentrated on the right bank and gradually shifting toward the left. The calculated RMSE and R^2 values validate the predictive capability of the ARIMA model used, with most sections showing R^2 values above 0.80. However, the shifting patterns are not uniform, suggesting site-specific drivers such as bank material, flow direction, and land use changes are in play (Hooke, 2007; Thakur et al., 2012). Altogether, the findings indicate that the Barak River is undergoing significant transformation in its urban stretch, driven by both natural geomorphic processes and rapid urban expansion. Channel shifting poses growing risks to infrastructure and settlements, highlighting the urgent need for integrated river management strategies. Monitoring using satellite imagery, combined with predictive modelling, offers an effective approach to anticipate future channel behaviour and design suitable interventions for sustainable river governance.

6. Conclusion

The study of the Barak River in the Silchar area indicates that there has been a distinct morphological/ land use change in the last three and a half decades. Channel width and migration have also increased steadily, mostly to the right bank in a number of sections. Meanwhile, the urban sprawl has caused settlement areas to increase at a significantly high rate at the expense of agricultural land and tall vegetation. These changes lead to the fact that people have more power over the river system, changing its natural flow and behaviour. The results show the importance of constant surveillance and long-term sustainable land use planning towards the mitigation of possible risks related to uncontrolled shifting of channels and massive urbanisation in riverbanks.

7. Future Recommendations

Following the outcomes of this research, it can be suggested that morphological and land use changes occurring in the Barak River and its urban reach in Silchar should be continuously observed with the help of satellite imagery and GIS-based methods. Buffer zones on both sides of the river should be created, which will limit the sources of human interference, and the river will have the freedom to change its course. There should be strict

regulations regarding urban sprawl, such as proper zoning to ensure that they do not take over flood plains, and floods and soil erosion will be minimised. Also, afforestation and re-establishment of riparian plants will be significant in stabilising the banks and keeping the ecology in check. Conservation can be enhanced through active community involvement and awareness creation methods, and integrated river basin management should involve the local governments, researchers and policymakers so that developmental necessities are balanced with the long-term sustainability of such a river system.

Declarations

"**Ethical Approval**: This study does not involve human or animal participants and therefore did not require ethical approval."

"**Consent to Participate**: Not applicable, as the study does not involve human participants."

"**Consent to Publish**: The author reported no potential conflict of interest."

"**Author's Contributions**: " WA contributed to writing the draft manuscript. WA reviewed and edited the draft."

"**Funding: "**No fund was provided".

"**Disclosure statement**: The author reported no potential conflict of interest."

"**Acknowledgement**: "The author acknowledges USGS for providing free satellite images."

"Clinical trial number"

Not applicable.'

References

1. Ackers P, Charlton FG (1970) Meander geometry arising from varying flows. J Hydrol 11(3):230–252
2. Annayat W (2025) Projection of IDF curves for the Barak River considering the effect of climate change. Int J Energy Water Resour, 1–19
3. Annayat W, Sil BS (2020a) Changes in morphometric meander parameters and prediction of meander channel migration for the alluvial part of the Barak River. J Geol Soc India 96(3):279–291
4. Annayat W, Sil BS (2020b) Assessing channel morphology and prediction of centerline channel migration of the Barak River using geospatial techniques. Bull Eng Geol Environ 79(10):5161–5183
5. Annayat W, Ashwini K, Sil BS (2022) Channel migration detection and landuse/landcover changes for Barak River in Northeast India. J Geol Soc India 98(7):981–990
6. Bag R, Mondal I, Bandyopadhyay J (2019) Assessing the oscillation of channel geometry and meander migration cardinality of Bhagirathi River, West Bengal, India. J Geog Sci 29(4):613–634
7. Congalton RG, Gu J, Yadav K, Thenkabail P, Ozdogan M (2014) Global land cover mapping: A review and uncertainty analysis. Remote Sens 6(12):12070–12093
8. Chang HH (1988) Fluvial Processes in River Engineering. Wiley, New York
9. Dabojani D, Mithun D, Kanti KK (2014, June) River change detection and bankline erosion recognition using remote sensing and GIS. Forum geografic 13(1):12–17
10. Daniel JF (1971) Channel movement of meandering Indiana streams, vol 732. US Government Printing Office
11. Da Silva Ferreira MA, Ebrahimi M (2017) Meandering morphodynamics. insights from laboratory and numerical experiments and beyond
12. Deb M, Das D, Uddin M (2012) Evaluation of meandering characteristics using RS & GIS of Manu River. J Water Resour Prot 4(3):163–171
13. Debnath J, Pan ND, Ahmed I, Bhowmik M (2017) Channel migration and its impact on land use/land cover using RS and GIS: a study on Khowai River of Tripura, North-East India. Egypt J Remote Sens Space Sci 20(2):197–210
14. Debnath J, Sahariah D, Saikia A, Meraj G, Nath N, Lahon D, Kanga S (2023) Shifting sands: assessing bankline shift using an automated approach in the Jia Bharali River, India. Land 12(3):703
15. Ferguson RI (1984) The threshold between meandering and braiding. Channels and Channel Control Structures. Springer, pp 749–763
16. Friedkin J (1945) A Laboratory Study of the Meandering of Alluvial Rivers. United States Waterways Experiment Station
17. Gilbert GK (1884) The sufficiency of terrestrial rotation for the deflection of streams. Am J Sci 3(162):427–432
18. Hazarika N, Das AK, Borah SB (2015) Assessing land-use changes driven by river dynamics in chronically flood affected Upper Brahmaputra plains, India, using RS-GIS techniques. Egypt J Remote Sens Space Sci 18(1):107–118
19. Hickin EJ (1977) The analysis of river-planform responses to changes in discharge. In *River Channel Changes* (pp. 249–263)
20. Hooke JM (2008) Temporal variations in fluvial processes on an active meandering river over a 20-year period. Geomorphology 100(1–2):3–13

21. Hooke JM, Harvey AM (1983) Meander changes in relation to bend morphology and secondary flows. Modern and Ancient Fluvial Systems. Wiley, pp 121–132
22. Howard AD, Dietrich WE, Seidl MA (1994) Modeling fluvial erosion on regional to continental scales. J Geophys Research: Solid Earth 99(B7):13971–13986
23. Inglis CC, Lacey G (1947) Meanders and their bearing on river training. Maritime Waterways Eng Div ICE Eng Div Papers 5(17):3–24
24. Islam A, Guchhait SK (2017) Analysing the influence of Farakka Barrage Project on channel dynamics and meander geometry of Bhagirathi River, West Bengal, India. Arab J Geosci 10(11):245
25. Jain SK, Agarwal PK, Singh VP (2007) Brahmaputra and Barak basin. Hydrology and Water Resources of India. Springer, pp 419–472
26. Jansen P, Van Bendegorn L, Van den Berg J, De Vries M, Zanen A (1979) *Principles of River Engineering: The Non-tidal Alluvial River*. Pitman
27. Khan MF, Annayat W, Venkateswarlu V (2025) Observations prediction riverbank erosion accretion from Landsat imagery and ARIMA model. Nat Hazards 121:10245
28. Klaassen GJ, Masselink G (1993) Planform changes of a braided river with fine sand as bed and bank material
29. Knighton AD (1999) Downstream variation in stream power. Geomorphology 29(3–4):293–306
30. Langbein WB, Leopold LB (1966) River meanders and the theory of minimum variance. Rivers and River Terraces. Palgrave Macmillan, pp 238–263
31. Lauer JW, Parker G (2008) Net local removal of floodplain sediment by river meander migration. Geomorphology 96(1–2):123–149
32. Leopold LB, Wolman MG (1960) River meanders. Geol Soc Am Bull 71(6):769–793
33. Leopold LB, Wolman MG (1957) River channel patterns: braided, meandering, and straight. US Government Printing Office
34. Lewin J, Brindle BJ (1977) Confined meanders. In *River Channel Changes* (pp. 221–233)
35. Martín-Vide JP, Andreatta A (2006) Disturbance caused by bed sills on the slopes of steep streams. J Hydraul Eng 132(11):1186–1194
36. Ondruch J, Máčka Z, Šulc Michalková M, Putiška R, Knot M, Holík P, Jenčo M (2018) Response of channel dynamics to recent meander neck cut-off in a lowland meandering river with artificial training history: the Morava River, Czech Republic. Hydrol Sci J 63(8):1236–1254
37. Onishi Y, Kennedy JF, Jain SC (1976) Effects of meandering in alluvial streams. J Hydraulic Div 102(7):899–917
38. Pan JJ, Chang CI (1992) Destriping of Landsat MSS images by filtering techniques. *Photogrammetric Engineering and Remote Sensing*
39. Rozovskii ILV (1957) *Flow of water in bends of open channels.*
40. Roy NG, Sinha R (2018) Integrating channel form and processes in the Gangetic plains rivers: Implications for geomorphic diversity. Geomorphology 302:46–61
41. Sil BS, Ashwini K, Annayat W, Debnath J, Farooq M, Meraj G (2022) Observing spatiotemporal inconsistency of erosion and accretion in the Barak River using remote sensing and GIS techniques. Conservation 3(1):14–31
42. Tiffany JB Jr, Nelson GA (1939) Studies of meandering of model-streams. Eos Trans Am Geophys Union 20(4):644–649
43. Thornes JB (1970) The hydraulic geometry of stream channels in the Xingu-Araguaia headwaters. Geographical J 136:376–382
44. Takagi T, Oguchi T, Matsumoto J, Grossman MJ, Sarker MH, Matin MA (2007) Channel braiding and stability of the Brahmaputra River, Bangladesh, since 1967: GIS and remote sensing analyses. Geomorphology 85:294–305
45. Thakur B et al (2012) Bank erosion and shifting of river channel: A case study of Ganga River. J Geomatics 6(2):93–100
46. Thorne CR, Lewin J (2020) Bank processes, bed material movement and planform development in a meandering river. Adjustments of the Fluvial System. Routledge, pp 117–137

Figures

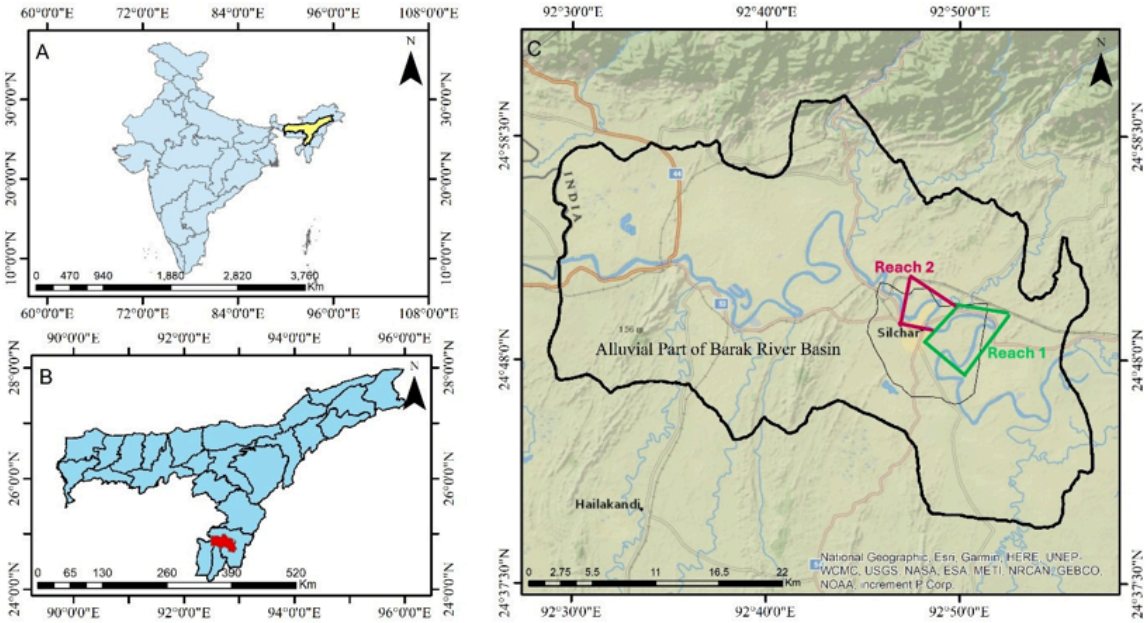


Figure 1

Map of the study area depicting the meandering section of the Barak River flowing through Silchar city in Assam, India. The map highlights major geomorphic features along the river corridor and marks specific observation points utilised for detailed analysis.

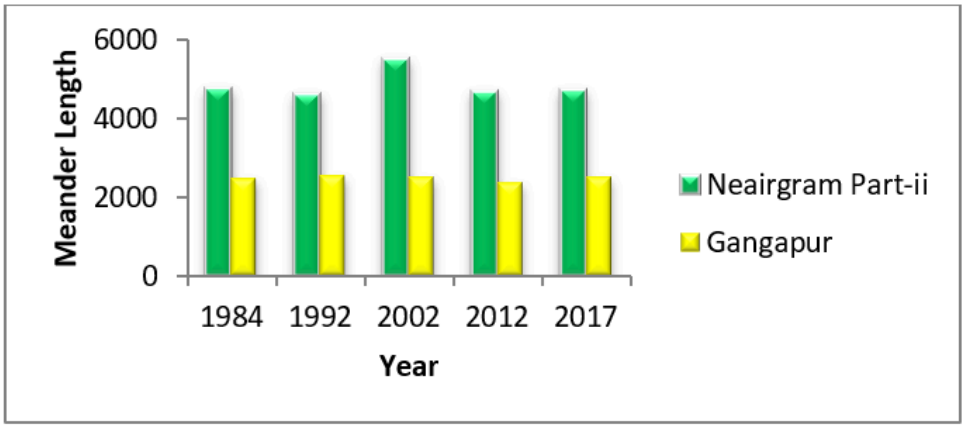


Figure 2

Temporal variation in meander length across study reaches of the Barak River.

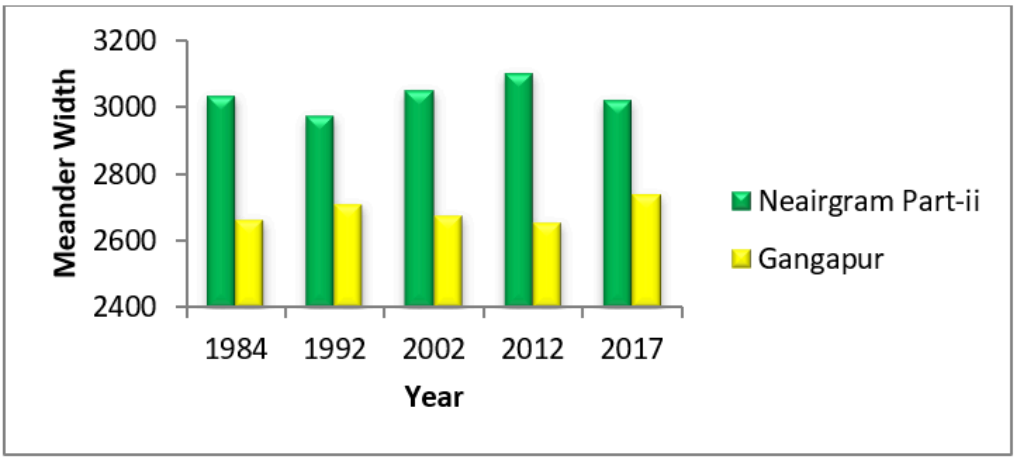


Figure 3

Temporal variation in meander width across study reaches of the Barak River

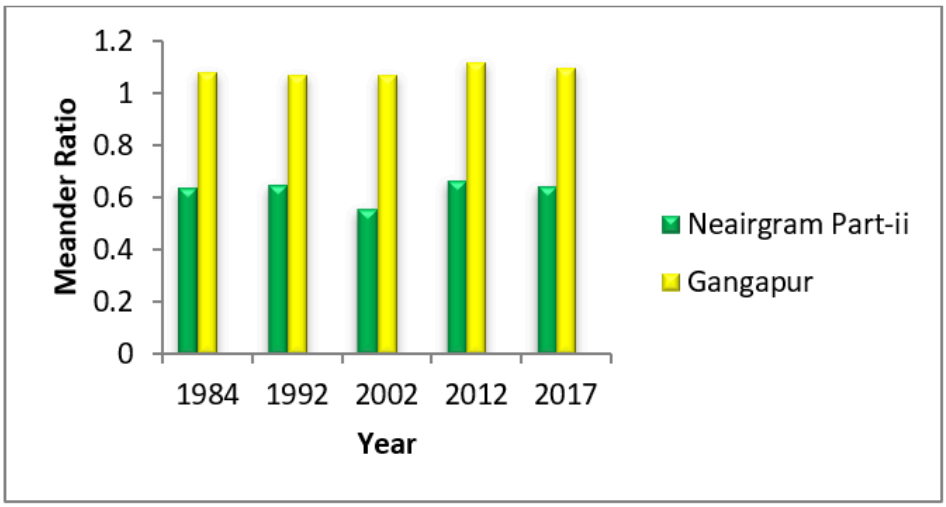


Figure 4

Temporal variation in meander ratio across study reaches of the Barak River

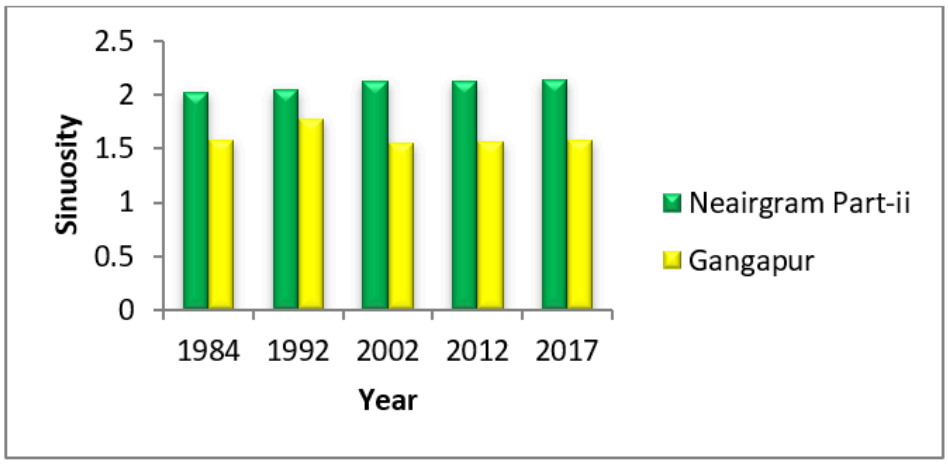


Figure 5

Temporal variation in sinuosity across study reaches of the Barak River

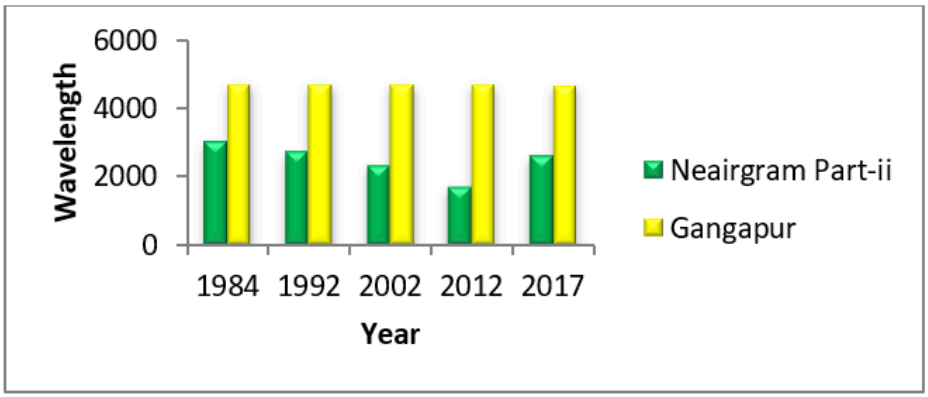


Figure 6

Temporal variation in wavelength across study reaches of the Barak River

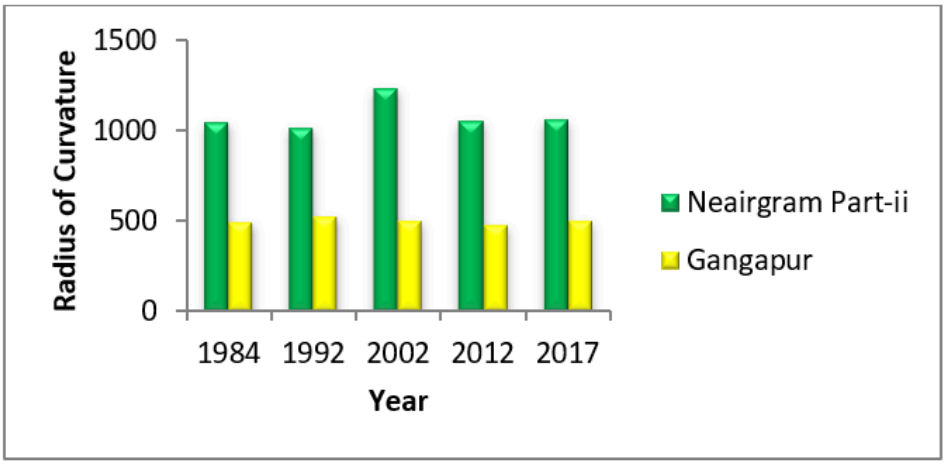


Figure 7

Temporal variation in radius of curvature across study reaches of the Barak River

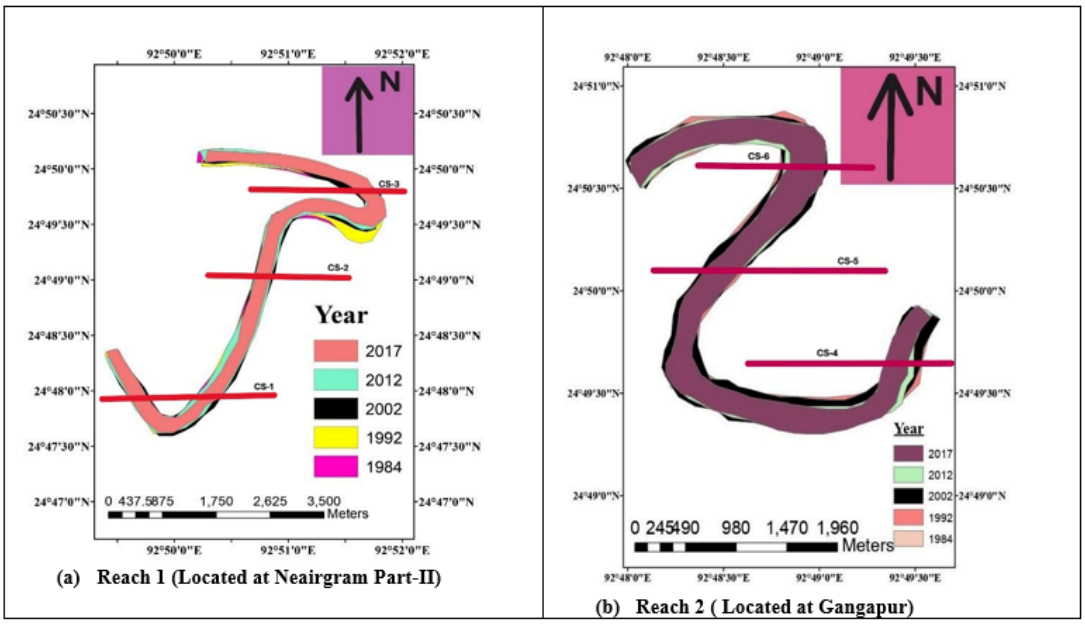


Figure 8

Map showing the temporal changes in river course from 1984 to 2017, illustrating channel migration and lateral shifting within the study area.

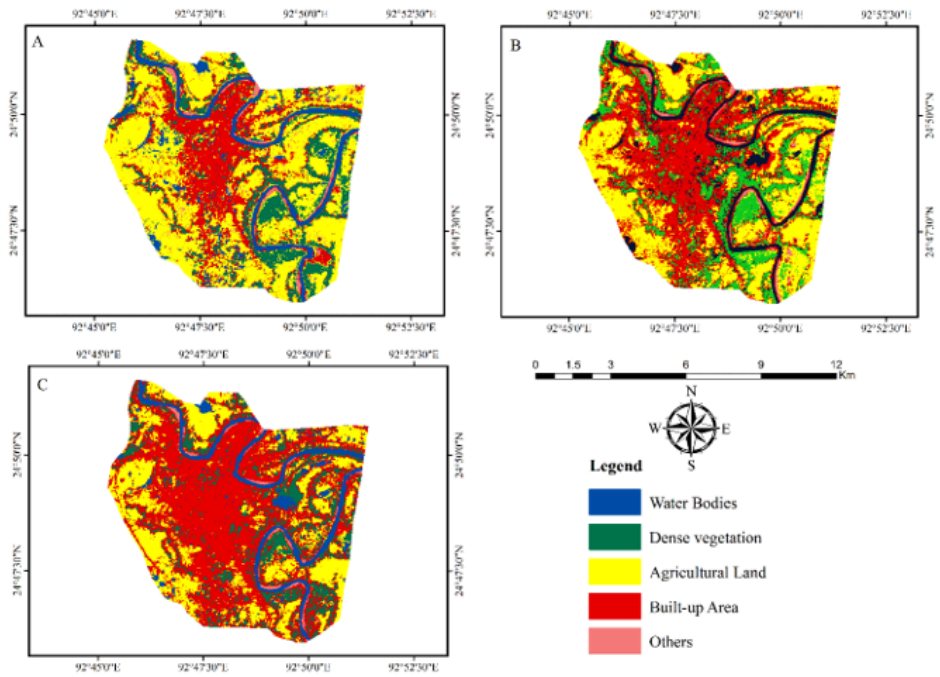


Figure 9

Land use and land cover maps of the study area for three different years: (A) 2000, (B) 2010, and (C) 2020. The maps classify features into water bodies, dense vegetation, agricultural land, built-up areas, and others, showing significant spatial changes over time

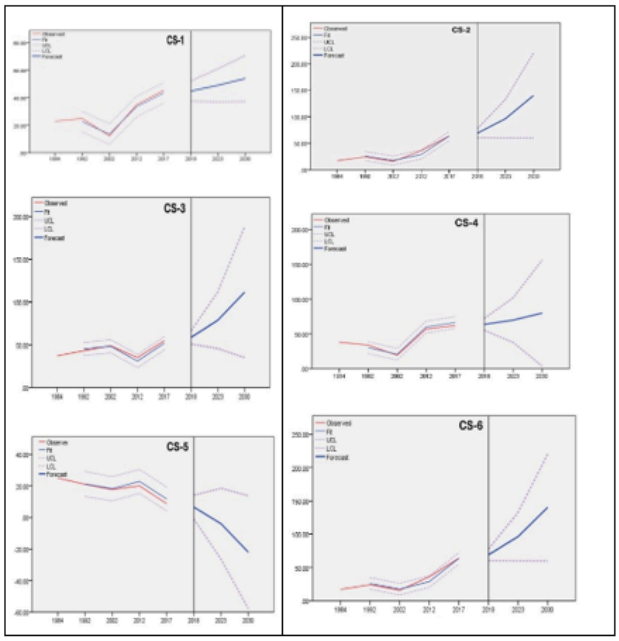


Figure 10

Changes in riverbank alignment between 1984 and 2030, indicating substantial migration of the left and right banks